

See discussions, stats, and author profiles for this publication at: <https://www.researchgate.net/publication/381313259>

# Fast simulation of the Kirchhoff–Carrier string with an energy–storing boundary condition using a Scalar Auxiliary Variable approach

Conference Paper · June 2024

CITATIONS

0

READS

79

4 authors:



**Michele Ducceschi**  
University of Bologna

75 PUBLICATIONS 448 CITATIONS

SEE PROFILE



**Alexis Mousseau**  
Université du Maine

3 PUBLICATIONS 0 CITATIONS

SEE PROFILE



**Stefan Bilbao**  
The University of Edinburgh

237 PUBLICATIONS 3,607 CITATIONS

SEE PROFILE



**Riccardo Russo**  
University of Bologna

16 PUBLICATIONS 13 CITATIONS

SEE PROFILE

# Fast simulation of the Kirchhoff-Carrier string with an energy-storing boundary condition using a Scalar Auxiliary Variable approach

Michele Ducceschi\* Alexis Mousseau\*\* Stefan Bilbao\*\*\*  
Riccardo Russo\*

\* *Department of Industrial Engineering, University of Bologna, Viale  
Risorgimento 2, Bologna, Italy*

*(e-mail: michele.ducceschi@unibo.it, riccardo.russo19@unibo.it)*

\*\* *Laboratoire d'Acoustique de l'Université du Mans (LAUM), UMR  
6613, Institut d'Acoustique - Graduate School (IA-GS), CNRS, Le  
Mans Université, France (e-mail: alexis.mousseau.etu@univ-lemans.fr)*

\*\*\* *Acoustics & Audio Group, University of Edinburgh, Edinburgh, UK  
(e-mail: sbilbao@ed.ac.uk)*

---

**Abstract:** Various string vibration models exist; linear models are common in musical acoustics but lack accuracy for complex phenomena. Nonlinear terms are necessary for pitch glides and modal couplings at higher amplitudes. Realistic boundary conditions are vital, often overlooked for simplicity. This study proposes an efficient time-stepping routine for nonlinear strings with energy-storing boundaries, derived from the Scalar Auxiliary Variable method, allowing fast inversion using the Sherman-Morrisson formula.

*Keywords:* Numerical Methods; Hamiltonian dynamics; Geometric mechanics.

---

## 1. INTRODUCTION

String vibration simulation encompasses a variety of computational methods employed to model and analyse the vibrational behaviour of strings; see, for instance, Chabassier et al. (2013); Bank and Sujbert (2005); Bilbao and Ducceschi (2023). Linear theory is insufficient to describe the physical and perceptual phenomena displayed by a vibrating string, as described by Morse and Ingard (1968); Gough (1984); Anand (1969). Various nonlinear models exist, and research works on the subject abound. The simplest nonlinear string model is due to Kirchhoff (1883), later formalised by Carrier (1945), incorporating a modulated tension term which is a function of the string's slope. This model describes some frequency-dependent phenomena, such as pitch glides, though it neglects the inherent coupling of the transverse and longitudinal motion, and was shown to be incorrect (Rowland (2011)). More refined models describing such coupling include a geometrically exact model (Chabassier and Joly (2010)), along with various approximations such as the one due to Morse and Ingard (1968).

Except for the Kirchhoff-Carrier model presenting an energy-conserving, explicit update presented by Bilbao and Smith (2005), the simulation of the distributed nonlinearity poses serious constraints concerning the choice of appropriate time-stepping routines. On one hand, respecting a form of energy conservation at the numerical level is necessary to guarantee the overall stability of the schemes; on the other hand, this has most often been accomplished

using implicit discretisations, see e.g. Chabassier and Joly (2010). These, ultimately, may represent a substantial computational bottleneck. These difficulties have been recently overcome by an application of the Scalar Auxiliary Variable (SAV) method introduced by Shen et al. (2018), for which an explicit, energy-conserving form exists for distributed potentials presenting a lower bound, as is the case for all the nonlinear models mentioned previously, as shown by Bilbao et al. (2023). Several concerns have been raised regarding the ability of SAV schemes to converge to the true solution of the associated differential problem, and numerical artefacts have been reported in various works, see e.g. Ducceschi and Bilbao (2019); Castera and Chabassier (2023); van Walstijn et al. (2024).

In a companion paper, an assessment of the SAV schemes for two nonlinear string potentials is carried out, highlighting a form of convergence in a series of benchmark tests (Russo et al. (2024)). This paper focuses on implementing a nonlinear string model comprising an energy-storing boundary condition at the bridge. This is a first step towards realising an impedance-like boundary condition, which can be measured experimentally and fitted using various methods in both the frequency and the time domain, such as those illustrated by Maestre et al. (2017); Bank and Karjalainen (2010); Ewins (2009). It will be shown that the update matrix is a  $2 \times 2$  block matrix where the diagonal blocks are rank-1 perturbations of diagonal matrices, and the off-diagonal blocks are rank-1. The inversion of the system's block matrix may then be performed efficiently by applying the Sherman and

Morrison (1950) formula repeatedly, yielding an explicit update. The article is structured as follows: Section 2 presents the continuous models of the nonlinear string coupled to the impedance boundary; Section 3 presents their discretisation within the SAV formalism; Section 4 presents a fast inversion formula of the update matrix and, finally, Section 5 presents a few numerical experiments, highlighting the ability of the current method to solve the nonlinear models efficiently.

## 2. CONTINUOUS MODELS

The inherent nonlinearity in the string will be modelled here by the simple Kirchhoff (1883) and Carrier (1945) term. It is known that this model is physically incorrect, as it neglects the coupling between the longitudinal and transverse polarisations altogether, see Rowland (2011). The model's simple form justifies its use in this work compared to more refined models such as the one by Morse and Ingard (1968), permitting a few algebraic manipulations to keep a compact notation, as will be shown shortly. Using a more refined nonlinear potential, one may still arrive at the results presented in the next section; in particular, the structure of the update matrix remains unchanged. For the sake of simplicity, losses, stiffness and external forcing are also neglected here.

Using the same notation as in the companion paper, the equation of motion of the sting is thus given as:

$$\rho A \partial_t^2 u = T_0 \partial_x^2 u + \mathcal{F}. \quad (1)$$

Here,  $u = u(x, t) : \mathcal{D} := [0, L] \times \mathbb{R}_0^+ \rightarrow \mathbb{R}$  represents the transverse displacement of a string of unstretched length  $L$ . It is a function of the spatial coordinate  $x$  and time  $t$ ;  $\partial_x^j$  and  $\partial_t^j$  represent the  $j$ -th partial derivative with respect of  $x$  and  $t$  respectively, and  $\mathcal{F} = \mathcal{F}(q)$  is a force density corresponding to the nonlinear contribution of the Kirchhoff-Carrier model. Here,  $q := \partial_x u$ .

In the following, the  $L_2$  inner product between functions  $p, q \in \mathcal{D}$  and related norm are defined as:

$$\langle p, q \rangle := \int_0^L pq \, dx, \quad \|q\| = \sqrt{\langle q, q \rangle}. \quad (2)$$

With this notation, the nonlinear force density for the Kirchhoff-Carrier model is expressed as:

$$\mathcal{F} = \partial_x \left( \frac{EA}{2L} \|q\|^2 q \right), \quad (3)$$

see e.g. Bilbao and Smith (2005). In the above, constants appear as  $\rho$ , the material density of the string (assumed constant along  $x$ );  $T_0$ , the applied tension;  $E$ , Young's modulus;  $A := \pi r_s^2$ , the area of the cross-section, with  $r_s$  the radius of the string.

Scaling the system by  $\rho A$ , using the form (3) in (1) and applying the definition of  $q$ , the equation of motion is written compactly as:

$$\partial_t^2 u = \partial_x (c^2 + \gamma \|q\|^2) q. \quad (4)$$

In the above,  $c := \sqrt{T_0/\rho A}$  is the linear wave speed;  $\gamma := E/2\rho L > 0$  is a parameter that determines the strength of the nonlinearity. Note that, in model (4), the nonlinear contributions are exclusively due to  $\|q\|$ : the net effect is an increase of the wave speed when the slope is not identically zero.

### 2.1 Energy-storing boundary formulation

An energy balance for model (4) is obtained immediately after taking an inner product of the equation with  $\partial_t u$ . Thus:

$$\langle \partial_t u, \partial_t^2 u \rangle = \langle \partial_t u, \partial_x (c^2 + \gamma \|q\|^2) q \rangle. \quad (5)$$

Integrating the right-hand side by parts, and using simple identities, one obtains the following:

$$\dot{\mathbb{H}}_{\mathcal{D}} = (\partial_t u (c^2 + \gamma \|q\|^2) q) \Big|_0^L, \quad (6)$$

where:

$$\mathbb{H}_{\mathcal{D}} := \frac{\|\partial_t u\|^2}{2} + \frac{c^2 \|q\|^2}{2} + \frac{\gamma \|q\|^4}{4}. \quad (7)$$

The overdot notation in (6) and in the following indicates total time differentiation. Thus, imposing Dirichlet conditions ( $u = 0$ ), or Neumann conditions ( $q = 0$ ) at either end, one recovers energy conservation, where the energy  $\mathbb{H}_{\mathcal{D}}$  is the sum of kinetic and potential contributions due to the string alone, here scaled by the linear density  $\rho A$ . In this work, a realistic and nontrivial boundary term is employed, with the boundary acting as an energy-storing device. This can be viewed as corresponding to a particular kind of boundary impedance without dissipation. Numerous works treat the problem of impedance end conditions, particularly in room acoustics, see e.g. Okuzono et al. (2021); Bilbao and Hamilton (2017); Hargreaves and Cox (2008). In all such cases, though, the problem in the domain interior is linear, whereas equation (6) implies a coupling of the string's inherent nonlinearity with the boundary term. To show this, first assume that the left endpoint is fixed, such that  $u(0, t) = 0 \forall t$ . Then, define  $f_L := (c^2 + \gamma \|q\|^2) q(L, t)$ . The right endpoint is assumed to satisfy the following:

$$\dot{\mathbf{z}} + \mathbf{G}\mathbf{z} = -\mathbf{b}f_L, \quad \mathbf{b}^\top \mathbf{z} = u(L, t) \quad (8)$$

Here,  $\mathbf{z} = \mathbf{z}(t) : \mathbb{R}_0^+ \rightarrow \mathbb{R}^N$  is an  $N \times 1$  vector, describing the time evolution of the boundary energy-storing elements;  $\mathbf{G} \in \mathbb{R}^{N \times N}$  is a positive, diagonal matrix;  $\mathbf{b} \in \mathbb{R}^N$  gives the participation factors of the boundary elements. Note that both  $\mathbf{G}$  and  $\mathbf{b}$  can be measured experimentally, by placing a sensor at the bridge and by fitting the impulse or frequency response with an appropriate mathematical model. They will be treated here as input (i.e. user-selectable) parameters along with  $N$ , the number of degrees of freedom of the boundary. The matrix  $\mathbf{G}$  can be thought of as collecting the squared resonant radian frequencies of the boundary elements, i.e.  $[\mathbf{G}]_{i,i} := \omega_i^2$ ,  $i = 1, \dots, N$ . The first equation in (8) is left-multiplied by  $\dot{\mathbf{z}}^\top$ , yielding:

$$\dot{\mathbf{z}}^\top \dot{\mathbf{z}} + \dot{\mathbf{z}}^\top \mathbf{G}\mathbf{z} = -\partial_t u(L, t) f_L, \quad (9)$$

where the second identity in (8) was used. Substituting this expression in (6), and using simple identities, one gets:

$$\dot{\mathbb{H}}_{\mathcal{D}} + \dot{\mathbb{H}}_{\mathcal{B}} = 0, \quad (10)$$

where the string's energy  $\mathbb{H}_{\mathcal{D}}$  is as in (7), and where the boundary energy is:

$$\mathbb{H}_{\mathcal{B}} := \frac{\dot{\mathbf{z}}^\top \dot{\mathbf{z}}}{2} + \frac{\mathbf{z}^\top \mathbf{G}\mathbf{z}}{2}. \quad (11)$$

Relation (10) expresses energy conservation of the string and the boundary terms altogether.

## 2.2 Energy Quadratisation

In view of the numerical scheme presented below, the equation of motion (4) and the related energy are written in terms of the *auxiliary variable*  $\psi$ , as:

$$\partial_t^2 u = \partial_x \left( c^2 + \sqrt{2\gamma} \psi \right) q, \quad \psi := \sqrt{\frac{\gamma}{2}} \|q\|^2. \quad (12)$$

Substituting the expression for  $\psi$  in (7), one gets:

$$\mathbf{H}_{\mathcal{D}} := \frac{\|\partial_t u\|^2}{2} + \frac{c^2 \|q\|^2}{2} + \frac{\psi^2}{2}, \quad (13)$$

and, thus, the energy comprises quadratic terms only. Note that  $\psi$  is here a *scalar* value, not a distributed quantity. The rate of change of  $\psi$  may itself be determined by deriving the second equation in (12):

$$\dot{\psi} = \sqrt{2\gamma} \langle q, \partial_t q \rangle. \quad (14)$$

This relationship, along with (12) and the related energy, forms the core of the SAV method (Shen et al. (2018)), allowing for a fast update of the associated numerical scheme, as shown in Bilbao et al. (2023). Before proceeding, note that the boundary force is expressed as:

$$f_L = \left( c^2 + \sqrt{2\gamma} \psi \right) q(L, t), \quad (15)$$

and, thus, includes a contribution of the auxiliary variable.

## 3. DISCRETE MODELS

The spatial component of the quadratised equation of motion is discretised first, followed by time discretisation. Both the semi- and fully discrete systems present an equivalent of the energy balance (10), from which stability may be inferred.

### 3.1 Spatial discretisation

The displacement  $u(x, t)$  will be approximated by a grid function  $u_m(t)$ , with  $m \in \mathcal{D} := [1, M] \subset \mathbb{N}$ . Equivalently, the grid function will be denoted in vector notation as  $\mathbf{u}(t) \in \mathbb{R}^M$ . The grid function is defined at equally spaced locations along  $\mathcal{D}$ , separated by the grid spacing  $h$ , with  $Mh = L$ . Thus, the grid function returns an approximation of the continuous displacement at the corresponding grid point:  $u_m(t) \approx u(mh, t)$ . Note that, in this notation,  $u_0(t)$  is excluded since a boundary condition of Dirichlet type is imposed at the left endpoint. The gradient  $q(x, t)$  is itself approximated by a grid function  $q_{m-\frac{1}{2}}$ ,  $m \in \mathcal{D}$ , where the half-integer notation denotes an interleaved-type grid function. This means that  $q_{m-\frac{1}{2}}(t) \approx q((m - \frac{1}{2})h, t)$ . The gradient will also be denoted in vector notation as  $\mathbf{q}(t)$ , again of length  $M$ . The grid functions are related as follows:

$$q_{\frac{1}{2}} = \frac{u_1}{h}, \quad q_{\frac{3}{2}} = \frac{u_2 - u_1}{h}, \quad \dots, \quad q_{m-\frac{1}{2}} = \frac{u_m - u_{m-1}}{h}. \quad (16)$$

The auxiliary variable  $\psi$  is defined as:

$$\psi = h \sqrt{\frac{\gamma}{2}} \mathbf{q}^\top \mathbf{q} \quad (17)$$

The boundary condition at the right endpoint, approximating (8) is given as follows:

$$\ddot{\mathbf{z}} + \mathbf{G}\mathbf{z} = -\mathbf{b}f_L, \quad \mathbf{b}^\top \mathbf{z} = u_M(t), \quad (18)$$

with the boundary force given as

$$f_L = \left( c^2 + \sqrt{2\gamma} \psi \right) q_{M+\frac{1}{2}}. \quad (19)$$

Given these definitions, the first equation in (12) is discretised as follows:

$$\ddot{u}_m = h^{-1} \left( c^2 + \sqrt{2\gamma} \psi \right) (q_{m+\frac{1}{2}} - q_{m-\frac{1}{2}}), \quad m = 1, \dots, M-1,$$

$$\ddot{u}_M = h^{-1} \left( f_L - \left( c^2 + \sqrt{2\gamma} \psi \right) q_{M-\frac{1}{2}} \right). \quad (20)$$

This system cannot be implemented directly, since the boundary force  $f_L$  is given in terms of  $q_{M+\frac{1}{2}}$ , which is undefined. Definitions of  $f_L$  including only interior grid points and  $\mathbf{z}$  can, however, be obtained easily. Left-multiplying the first equation in (18) by  $\mathbf{b}^\top$  one gets:

$$f_L = -(\mathbf{b}^\top \mathbf{b})^{-1} (\ddot{\mathbf{z}} + \mathbf{G}\mathbf{z}). \quad (21)$$

A second expression for the boundary force may be obtained by substituting the second identity in (18) into (20):

$$f_L = h \mathbf{b}^\top \ddot{\mathbf{z}} + \left( c^2 + \sqrt{2\gamma} \psi \right) q_{M-\frac{1}{2}}. \quad (22)$$

The rate of change of  $\psi$  may itself be obtained from (14), as:

$$\dot{\psi} = h \sqrt{2\gamma} \mathbf{q}^\top \dot{\mathbf{q}}. \quad (23)$$

It is convenient, at this point, to collect all the equations of motion compactly in vector form. To that end, substitute expression (21) in (20), and expression (22) in (18). Using the definition of  $q_{m-\frac{1}{2}}$  from (16), a system comprising  $M + N + 1$  equations is obtained as:

$$\ddot{\mathbf{u}} = \left( c^2 + \sqrt{2\gamma} \psi \right) \mathbf{D}^2 \mathbf{u} - \frac{\hat{\mathbf{e}}_M \mathbf{b}^\top}{h \mathbf{b}^\top \mathbf{b}} (\ddot{\mathbf{z}} + \mathbf{G}\mathbf{z}), \quad (24a)$$

$$(\mathbf{I}_z + h \mathbf{b} \mathbf{b}^\top) \ddot{\mathbf{z}} = -\mathbf{G}\mathbf{z} - \mathbf{b} \left( c^2 + \sqrt{2\gamma} \psi \right) q_{M-\frac{1}{2}}, \quad (24b)$$

$$\dot{\psi} = -h \sqrt{2\gamma} (\mathbf{D}^2 \mathbf{u})^\top \dot{\mathbf{u}}. \quad (24c)$$

In the above, the discrete Laplacian, a symmetric operator of dimension  $M \times M$ , was introduced as:

$$\mathbf{D}^2 = h^{-2} \text{diag}([1, -2, 1]), \quad (25)$$

and furthermore:

$$\hat{\mathbf{e}}_M := [0, 0, \dots, 0, 1]^\top \quad (26)$$

is the  $M^{\text{th}}$  Euclidian basis vector in  $\mathbb{R}^M$ .

System (24) respects an energy balance analogous to (10) in the continuous case. Here, though, the semi-discrete string energy is given as:

$$\mathbf{H}_{\mathcal{D}} := \frac{h \dot{\mathbf{u}}^\top \dot{\mathbf{u}}}{2} - \frac{c^2 h}{2} \mathbf{u}^\top \mathbf{D}^2 \mathbf{u} + \frac{\psi^2}{2}. \quad (27)$$

The energy expression for the boundary energy remains formally unchanged so that:

$$\mathbf{H}_{\mathfrak{B}} := \frac{\dot{\mathbf{z}}^\top \dot{\mathbf{z}}}{2} + \frac{\mathbf{z}^\top \mathbf{G}\mathbf{z}}{2}. \quad (28)$$

Thus, the semi-discrete energy balance is:

$$\dot{\mathbf{H}}_{\mathcal{D}} + \dot{\mathbf{H}}_{\mathfrak{B}} = 0. \quad (29)$$

Note that the total energy is a quadratic form, mimicking the expression of the continuous energy. The string energy (27), in particular, is non-negative because the Laplace operator  $\mathbf{D}^2$  is negative-definite. Its eigenvalues are found in the range:

$$-4h^{-2} \leq \lambda_{\mathbf{D}^2} < 0. \quad (30)$$

This condition allows to bound the total energy from below.

### 3.2 Temporal discretisation

An appropriate time discretisation will now be derived for system (24). Many choices are available. Here, the scheme is designed following these principles: the linear part of the string is discretised *explicitly* in the domain interior. An implicit discretisation is, however, used at the boundary: this allows incorporating an arbitrary number of boundary elements without affecting the stability properties of the string's own discretisation. Finally, the nonlinear part will be discretised according to the SAV framework. Thus, the grid function  $\mathbf{u}(t)$  is approximated by a time series  $\mathbf{u}^n$ , where  $n$  is the time index. The approximation is such that  $\mathbf{u}^n \approx \mathbf{u}(nk)$ , where  $k$ , the time step, is the multiplicative inverse of the input sample rate. The gradient  $\mathbf{q}$  will also be approximated on the same discrete-time axis, so that  $\mathbf{q}^n \approx \mathbf{q}(nk)$ . The boundary terms  $\mathbf{z}$  are discretised in time following the same principle, so that  $\mathbf{z}^n \approx \mathbf{z}(nk)$ . The auxiliary variable will instead be evaluated on an interleaved time axis, as  $\psi^{n-\frac{1}{2}} \approx \psi((n-\frac{1}{2})k)$ .

Following the notation in the companion paper, time-difference operators are given as:

$$\delta_{\pm}\mathbf{u}^n := \pm \frac{\mathbf{u}^{n\pm 1} - \mathbf{u}^n}{k}, \quad \delta\mathbf{u}^n := \frac{1}{2}(\delta_+ + \delta_-)\mathbf{u}^n. \quad (31)$$

The second time difference is obtained as:

$$\delta_2\mathbf{u}^n := \frac{1}{k}(\delta_+ - \delta_-)\mathbf{u}^n. \quad (32)$$

An analogous definition holds when the operator  $\delta_2$  is applied to the boundary time series  $\mathbf{z}^n$ . Difference operators acting on the interleaved time series  $\psi$  are defined similarly; in particular:

$$\delta_{\pm}\psi^{n-\frac{1}{2}} := \frac{\psi^{n+\frac{1}{2}} - \psi^{n-\frac{1}{2}}}{k}. \quad (33)$$

Averaging operators will also be used. Two, in particular, are given here as:

$$\mu\mathbf{z}^n := \frac{\mathbf{z}^{n-1} + \mathbf{z}^{n+1}}{2}, \quad \mu + \psi^{n-\frac{1}{2}} := \frac{\psi^{n+\frac{1}{2}} + \psi^{n-\frac{1}{2}}}{2}. \quad (34)$$

Some useful identities can be derived from the definitions above. Three, in particular, will be used later:

$$\delta = \frac{k}{2}\delta_2 + \delta_-, \quad \mu = \frac{k^2}{2}\delta_2 + 1, \quad \mu_+ = \frac{k}{2}\delta_+ + 1. \quad (35)$$

With this in mind, a time discretisation of system (24) is given as:

$$\begin{aligned} \delta_2\mathbf{u}^n &= \left(c^2 + \sqrt{2\gamma}\mu_+\psi^{n-\frac{1}{2}}\right)\mathbf{D}^2\mathbf{u}^n - \\ &\quad - \frac{\hat{\mathbf{e}}_M\mathbf{b}^\top}{h\mathbf{b}^\top\mathbf{b}}(\delta_2\mathbf{z}^n + \mathbf{G}\mu\mathbf{z}^n), \end{aligned} \quad (36a)$$

$$\begin{aligned} (\mathbf{I}_z + h\mathbf{b}\mathbf{b}^\top)\delta_2\mathbf{z}^n &= -\mathbf{G}\mu\mathbf{z}^n - \\ &\quad - \mathbf{b}\left(c^2 + \sqrt{2\gamma}\mu_+\psi^{n-\frac{1}{2}}\right)q_{M-\frac{1}{2}}^n, \end{aligned} \quad (36b)$$

$$\delta_+\psi^{n-\frac{1}{2}} = -h\sqrt{2\gamma}(\mathbf{D}^2\mathbf{u}^n)^\top\delta\mathbf{u}^n. \quad (36c)$$

The scheme is conservative. For the sake of conciseness, a proof will be omitted, and the result is simply stated. As for the continuous and semi-discrete cases, the energy balance comprises a string term and a boundary term, and is:

$$\delta_+\mathfrak{H}_{\mathfrak{D}}^{n-\frac{1}{2}} + \delta_+\mathfrak{H}_{\mathfrak{B}}^{n-\frac{1}{2}} = 0, \quad (37)$$

where

$$\begin{aligned} \mathfrak{H}_{\mathfrak{D}}^{n-\frac{1}{2}} &:= \frac{h(\delta_-\mathbf{u}^n)^\top(\delta_-\mathbf{u}^n)}{2} - \frac{c^2h}{2}(\mathbf{u}^n)^\top\mathbf{D}^2\mathbf{u}^{n-1} + \frac{(\psi^{n-\frac{1}{2}})^2}{2}, \\ \mathfrak{H}_{\mathfrak{B}}^{n-\frac{1}{2}} &:= \frac{(\delta_-\mathbf{z}^n)^\top(\delta_-\mathbf{z}^n)}{2} + \frac{(\mathbf{z}^n)^\top\mathbf{G}\mathbf{z}^n}{4} + \frac{(\mathbf{z}^{n-1})^\top\mathbf{G}\mathbf{z}^{n-1}}{4}. \end{aligned}$$

Note that the boundary energy  $\mathfrak{H}_{\mathfrak{B}}^{n-\frac{1}{2}}$  is non-negative at all times, and so is the nonlinear energy in  $\mathfrak{H}_{\mathfrak{D}}^{n-\frac{1}{2}}$  expressed via the square of the auxiliary function. These properties are a direct consequence of the use of the averaging operators  $\mu$  and  $\mu_+$  applied to  $\mathbf{z}$  and  $\psi$  in (36).

In light of this, the non-negativity of the energy overall will be determined by the non-negativity of the linear part of  $\mathfrak{H}_{\mathfrak{D}}^{n-\frac{1}{2}}$ . This can be obtained easily using bounds (30) and simple identities. The result is the usual CFL (Courant et al. (1967)) condition for the linear wave equation:

$$ck \leq h. \quad (38)$$

Enforcing this condition allows bounding the fully discrete energy from below, guaranteeing a form of stability.

## 4. A FAST INVERSION ALGORITHM

Scheme (36) appears to have an implicit form, representing a severe computational bottleneck. However, it possesses a useful structure for which a fast update may be derived. The enabling idea is to perform the update by blocks, where each block has the structure of a diagonal matrix plus a rank-one perturbation. These matrices are clearly invertible and possess a fast inversion formula, according to Sherman and Morrison (1950):

$$(\mathbf{A} + \boldsymbol{\alpha}\boldsymbol{\beta}^\top)^{-1} = \mathbf{A}^{-1} - \frac{\mathbf{A}^{-1}\boldsymbol{\alpha}\boldsymbol{\beta}^\top\mathbf{A}^{-1}}{1 + \boldsymbol{\beta}^\top\mathbf{A}^{-1}\boldsymbol{\alpha}}. \quad (39)$$

First, it is convenient to eliminate  $\psi^{n+\frac{1}{2}}$  from (36a) and (36b). To that end, the third identity in (35) gives:

$$\mu_+\psi^{n-\frac{1}{2}} = -\frac{hk}{2}\sqrt{2\gamma}(\mathbf{D}^2\mathbf{u}^n)^\top\delta\mathbf{u}^n + \psi^{n-\frac{1}{2}}. \quad (40)$$

Note that the  $\delta$  can itself be recast using the first identity in (35). Thus:

$$\mu_+\psi^{n-\frac{1}{2}} = -\frac{hk}{2}\sqrt{2\gamma}(\mathbf{D}^2\mathbf{u}^n)^\top\left(\frac{k}{2}\delta_2 + \delta_-\right)\mathbf{u}^n + \psi^{n-\frac{1}{2}}.$$

This expression is substituted in (36a) and (36b), effectively eliminating the dependence of these equations on  $\psi^{n+\frac{1}{2}}$ . Then, the second identity in (35) is used in (36a) and (36b), so that:

$$\mu\mathbf{z}^n = \frac{k^2}{2}\delta_2\mathbf{z}^n + \mathbf{z}^n. \quad (41)$$

Now, (36a) and (36b) can be written as:

$$\mathbf{A}^n \begin{bmatrix} \delta_2\mathbf{u}^n \\ \delta_2\mathbf{z}^n \end{bmatrix} = \begin{bmatrix} \boldsymbol{\zeta}_{\mathbf{u}}^n \\ \boldsymbol{\zeta}_{\mathbf{z}}^n \end{bmatrix}. \quad (42)$$

Above, the vectors  $\boldsymbol{\zeta}_{\mathbf{u}}^n$  and  $\boldsymbol{\zeta}_{\mathbf{z}}^n$  have known expressions, omitted here for brevity. Furthermore, the time-dependent matrix  $\mathbf{A}$  is a block matrix:

$$\mathbf{A} := \begin{bmatrix} \mathbf{A}_{uu} & \mathbf{A}_{uz} \\ \mathbf{A}_{zu} & \mathbf{A}_{zz} \end{bmatrix}, \quad (43)$$

where the diagonal blocks are square matrices of dimension, respectively,  $M \times M$  and  $N \times N$ . The off-diagonal blocks have consistent dimensions:  $M \times N$  and  $N \times M$ .

Thus, to compute the unknown accelerations, one must invert  $\mathbf{A}$ :

$$\begin{bmatrix} \delta_2 \mathbf{u}^n \\ \delta_2 \mathbf{z}^n \end{bmatrix} = \mathbf{A}^{-1} \begin{bmatrix} \zeta_u^n \\ \zeta_z^n \end{bmatrix}. \quad (44)$$

It is assumed that  $\mathbf{u}^n, \mathbf{u}^{n-1}, \mathbf{z}^n, \mathbf{z}^{n-1}$  are known. Hence, once the system is inverted, one obtains:

$$\begin{aligned} \mathbf{u}^{n+1} &= k^2 \delta_2 \mathbf{u}^n + 2\mathbf{u}^n - \mathbf{u}^{n-1}, \\ \mathbf{z}^{n+1} &= k^2 \delta_2 \mathbf{z}^n + 2\mathbf{z}^n - \mathbf{z}^{n-1}. \end{aligned}$$

The auxiliary variable is then updated immediately via (36c).

#### 4.1 Block inversion

From linear algebra, one has:

$$\mathbf{A}^{-1} = \mathbf{S}^{-1} \begin{bmatrix} \mathbf{I}_u & -\mathbf{A}_{uz} \mathbf{A}_{zz}^{-1} \\ -\mathbf{A}_{zu} \mathbf{A}_{uu}^{-1} & \mathbf{I}_z \end{bmatrix} \quad (45)$$

where

$$\mathbf{S} = \begin{bmatrix} \mathbf{A}_{uu} - \mathbf{A}_{uz} \mathbf{A}_{zz}^{-1} \mathbf{A}_{zu} & \mathbf{0} \\ \mathbf{0} & \mathbf{A}_{zz} - \mathbf{A}_{zu} \mathbf{A}_{uu}^{-1} \mathbf{A}_{uz} \end{bmatrix} \quad (46)$$

contains the Schur complements of  $\mathbf{A}_{uu}$  and  $\mathbf{A}_{zz}$  within  $\mathbf{A}$ . This formula is convenient as it allows using the Sherman-Morrison formula (39) repeatedly. First, note that the form of the diagonal blocks is as follows:

$$\mathbf{A}_{uu} := \mathbf{I}_u + \frac{\gamma h k^2}{2} \mathbf{s} \mathbf{s}^\top, \quad \mathbf{A}_{zz} := \mathbf{W} + h \mathbf{b} \mathbf{b}^\top, \quad (47)$$

with  $\mathbf{s} := \mathbf{D}^2 \mathbf{u}^n$ ,  $\mathbf{W} := \mathbf{I}_z + \frac{k^2}{2} \mathbf{G}$ . Hence, both blocks are both in the form of a diagonal matrix plus a rank-one perturbation (remember that  $\mathbf{G}$  is itself diagonal). The off-diagonal blocks have the form:

$$\mathbf{A}_{uz} := \frac{\hat{\mathbf{e}}_M \mathbf{d}^\top}{h \mathbf{b}^\top \mathbf{b}}, \quad \mathbf{A}_{zu} := -\frac{\gamma h k^2 q_{M-\frac{1}{2}}^n}{2} \mathbf{b} \mathbf{s}^\top, \quad (48)$$

where  $\mathbf{d} := \mathbf{W} \mathbf{b}$ .

In order to invert system (44), one uses (45) in (44). Hence, one first computes:

$$\begin{bmatrix} \chi_u^n \\ \chi_z^n \end{bmatrix} = \begin{bmatrix} \mathbf{I}_u & -\mathbf{A}_{uz} \mathbf{A}_{zz}^{-1} \\ -\mathbf{A}_{zu} \mathbf{A}_{uu}^{-1} & \mathbf{I}_z \end{bmatrix} \begin{bmatrix} \zeta_u^n \\ \zeta_z^n \end{bmatrix}. \quad (49)$$

This can be achieved quickly by inverting  $\mathbf{A}_{uu}$ ,  $\mathbf{A}_{zz}$  using (39). Once these are computed, the accelerations are obtained as:

$$\delta_2 \mathbf{u}^n = (\mathbf{A}_{uu} - \mathbf{A}_{uz} \mathbf{A}_{zz}^{-1} \mathbf{A}_{zu})^{-1} \chi_u^n, \quad (50a)$$

$$\delta_2 \mathbf{z}^n = (\mathbf{A}_{zz} - \mathbf{A}_{zu} \mathbf{A}_{uu}^{-1} \mathbf{A}_{uz})^{-1} \chi_z^n. \quad (50b)$$

The inversion of the Shur complements can once again be accomplished using (39), since these are themselves in the form of rank-1 perturbations of diagonal matrices. A proof is now given for (50b), with a similar proof holding for (50a). First, compute:

$$\mathbf{A}_{uu}^{-1} \mathbf{A}_{uz} = \frac{1}{h \mathbf{b}^\top \mathbf{b}} \left( \hat{\mathbf{e}}_M - \frac{\gamma h k^2 s_M}{2 + \gamma h k^2 \mathbf{s}^\top \mathbf{s}} \mathbf{s} \right) \mathbf{d}^\top, \quad (51)$$

where  $s_M := (\mathbf{s})_M$ . Hence:

$$\mathbf{A}_{zu} \mathbf{A}_{uu}^{-1} \mathbf{A}_{uz} = -\frac{\gamma k^2 s_M q_{M-\frac{1}{2}}}{\mathbf{b}^\top \mathbf{b} (2 + \gamma h k^2 \mathbf{s}^\top \mathbf{s})} \mathbf{b} \mathbf{d}^\top$$

From the above, define:

$$\mathbf{g} := h \mathbf{b} + \frac{\gamma k^2 s_M q_{M-\frac{1}{2}}}{\mathbf{b}^\top \mathbf{b} (2 + \gamma h k^2 \mathbf{s}^\top \mathbf{s})} \mathbf{d}. \quad (52)$$

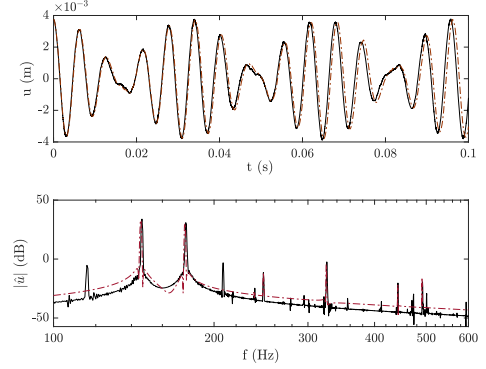


Fig. 1. Example time and frequency domain plots of a nonlinear string using  $N = 100$  boundary elements. The string is initialised in the first eigenmode of a fixed-fixed string, with a maximum amplitude of 5 mm. The plots compare the Kirchhoff-Carrier (solid black) and fully linear (dashed magenta) cases. The output is recorded at  $x_o = 0.73L$ .

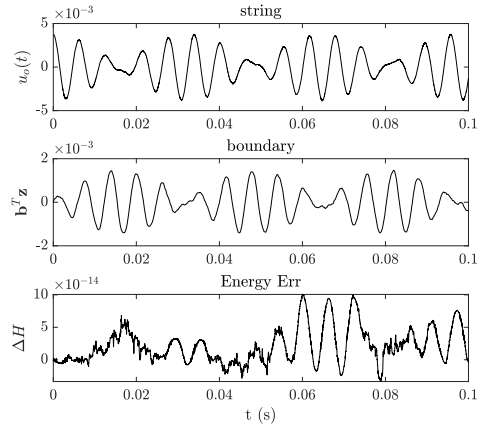


Fig. 2. Time domain plot of the nonlinear string, for the same string as Figure 1. The displacements of the string at the output location and of the boundary are given, along with the energy error.

Thus, using these in (50b) results in the following expression:

$$\delta_2 \mathbf{z}^n = (\mathbf{W} + \mathbf{b} \mathbf{g}^\top)^{-1} \chi_z^n, \quad (53)$$

which may again be inverted efficiently using (39).

## 5. NUMERICAL RESULTS

A comparison between the linear and nonlinear dynamics is offered in Figure 1. The string is initialised, in this case, in the first eigenmode of the corresponding fixed-fixed string, with an amplitude of 5 mm. The increased wave speed in the nonlinear case is visible in the time domain plot, where the wavefronts appear to travel faster. The same phenomenon is visible in the frequency domain plot, where the resonance peaks in the nonlinear case are shifted to the right, highlighting an increased vibration frequency. Note the presence of further peaks here: these are produced by the coupling between the boundary and the string's nonlinearity. An example of the energy conservation of the scheme is given in Figure 2: note that the error is

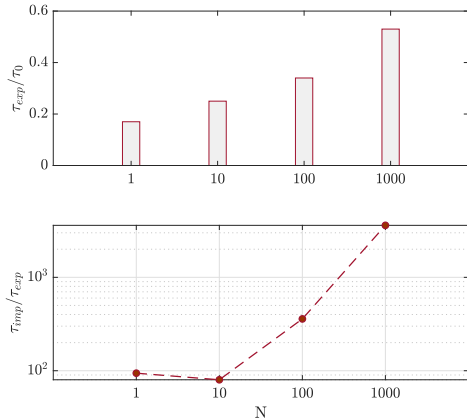


Fig. 3. Matlab compute times of the fast algorithm ( $\tau_{exp}$ ) and Matlab’s own backslash ( $\tau_{imp}$ ), as a function of  $N$ , the number of boundary elements. Top:  $\tau_{exp}$  as a fraction of real-time  $\tau_0$  for the nonlinear string of Figure 1. Bottom  $\tau_{imp}/\tau_{exp}$ . For all simulations, the time step is  $k = 1/44100$  s, corresponding to  $M = 133$ . The tests were run on an Apple M2 Pro chip.

of the order of machine accuracy over thousands of time steps, as per (37). Finally, the Matlab compute times of the fast algorithm  $\tau_{exp}$  are reported in Figure 3. Note that, as expected, the compute time scale with  $N$ , the number of boundary elements. However, the algorithm can compute thousands of nonlinearly coupled degrees of freedom well below real-time, highlighting the efficiency of the proposed algorithm. A comparison against Matlab’s own “backslash” solver is given in the same Figure. The solver is used directly on system (44), without any optimisation. Note that, as the number  $N$  of boundary elements grows, the time ratio between the two schemes becomes exponentially bigger, and gains of the order of three orders of magnitude are recovered.

## 6. CONCLUSIONS

This article illustrated a method to treat the problem of a nonlinear string presenting a kind of impedance boundary. A time discretisation of the string’s own nonlinearity was given in terms of the Scalar Auxiliary Variable method; the boundary condition was discretised using temporal averaging operators. The resulting scheme is characterised by a classic CFL stability condition. The structure of the scheme’s update matrix was thoroughly investigated, and a fast inversion algorithm was given in terms of a repeated application of the Sherman-Morrison inversion formula. Matlab benchmark tests showed consistent speedups, up to three orders of magnitude for larger systems.

## ACKNOWLEDGEMENTS

This work was supported by the European Research Council (ERC), under grant 2020-StG-950084-NEMUS.

## REFERENCES

Anand, G. (1969). Large-amplitude damped free vibration of a stretched string. *J Acoust Soc Am*, 45(5), 1089–1096.

- Bank, B. and Karjalainen, M. (2010). Passive admittance matrix modeling for guitar synthesis. In *Proc. Digital Audio Effects (DAFx-10)*. Graz, Austria.
- Bank, B. and Sujbert, L. (2005). Generation of longitudinal vibrations in piano strings: From physics to sound synthesis. *J Acoust Soc Am*, 117, 2268–2278.
- Bilbao, S. and Ducceschi, M. (2023). Models of musical string vibration. *Acoust Sc Tech*, 44(3), 194–209.
- Bilbao, S., Ducceschi, M., and Zama, F. (2023). Explicit exactly energy-conserving methods for hamiltonian systems. *J Comput Phys*, 472, 111697.
- Bilbao, S. and Hamilton, B. (2017). Wave-based room acoustics simulation: Explicit/implicit finite volume modeling of viscothermal losses and frequency-dependent boundaries. *J Audio Eng Soc*, 65(1/2), 78–89.
- Bilbao, S. and Smith, J. (2005). Energy-conserving finite difference schemes for nonlinear strings. *Acta Acust United Acust*, 91, 299–311.
- Carrier, G. (1945). On the non-linear vibration problem of the elastic string. *Quart Appl Math*, 3(2), 157–165.
- Castera, G. and Chabassier, J. (2023). Numerical analysis of quadratized schemes. Application to the simulation of the nonlinear piano string. Technical Report RR-9516, Inria.
- Chabassier, J., Chaigne, A., and Joly, P. (2013). Modeling and simulation of a grand piano. *J Acoust Soc Am*, 134, 648–665.
- Chabassier, J. and Joly, P. (2010). Energy preserving schemes for nonlinear hamiltonian systems of wave equations: Application to the vibrating piano string. *Comp Met Appl Mech Eng*, 199(45), 2779–2795.
- Courant, R., Friedrichs, K., and Lewy, H. (1967). On the partial difference equations of mathematical physics. *IBM J Res Dev*, 11(2), 215–234.
- Ducceschi, M. and Bilbao, S. (2019). Non-iterative solvers for nonlinear problems: the case of collisions. In *Proc. Digital Audio Effects (DAFx-19)*. Birmingham, UK.
- Ewins, D.J. (2009). *Modal testing: theory, practice and application*. John Wiley & Sons.
- Gough, C. (1984). The nonlinear free vibration of a damped elastic string. *J Acoust Soc Am*, 75(6), 1770–1776.
- Hargreaves, J.A. and Cox, T.J. (2008). A transient boundary element method model of schroeder diffuser scattering using well mouth impedance. *J Acoust Soc Am*, 124(5), 2942–2951.
- Kirchhoff, G. (1883). *Vorlesungen über Mechanik*. Tauber, Leipzig.
- Maestre, E., Scavone, G.P., and Smith, J.O. (2017). Joint modeling of bridge admittance and body radiativity for efficient synthesis of string instrument sound by digital waveguides. *IEEE/ACM Trans Audio Speech Lang Proc*, 25(5), 1128–1139.
- Morse, P. and Ingard, U. (1968). *Theoretical Acoustics*. Princeton University Press, Princeton, NJ, USA.
- Okuzono, T., Yoshida, T., and Sakagami, K. (2021). Efficiency of room acoustic simulations with time-domain fem including frequency-dependent absorbing boundary conditions: Comparison with frequency-domain FEM. *Appl Acoust*, 182, 108212.
- Rowland, D.R. (2011). The potential energy density in transverse string waves depends critically on longitudinal motion. *Eur J Phys*, 32(6), 1475.
- Russo, R., Bilbao, S., and Ducceschi, M. (2024). Scalar auxiliary variable techniques for nonlinear transverse string vibration. In *8th IFAC Workshop on Lagrangian and Hamiltonian Methods for Non Linear Control*. Besançon, France.
- Shen, J., Xu, J., and Yang, J. (2018). The scalar auxiliary variable (SAV) approach for gradient flows. *J Comput Phys*, 353, 407–416.
- Sherman, J. and Morrison, W.J. (1950). Adjustment of an inverse matrix corresponding to a change in one element of a given matrix. *Ann Math Stat*, 21, 124–127.
- van Walstijn, M., Chatziioannou, V., and Bhanuprakash, A. (2024). Implicit and explicit schemes for energy-stable simulation of string vibrations with collisions: Refinement, analysis, and comparison. *J Sound Vib*, 569, 117968.